

Generation of indistinguishable single photons and polarization-entangled photon-pairs via polaritonic superfluid to Mott-insulator quantum phase transition

Neil Na¹ and Yoshihisa Yamamoto^{1,2}

¹*E. L. Ginzton Laboratory, Stanford University, Stanford, California 94305, USA*

²*National Institute of Informatics, Hitotsubashi, Chiyoda-ku, Tokyo 101-8430, Japan*

We show theoretically the superfluid to Mott-insulator quantum phase transition in an array of exciton-polariton traps can be utilized for massive parallel generation of indistinguishable single photons and polarization-entangled photon-pairs. We exhibit our proposal on a periodically modulated semiconductor planar microcavity with realistic experimental parameters. By means of analytical and numerical methods, the device operation and its robustness against system imperfection are studied. Such a deterministic single photon and entangled photon-pair generation may open up a new perspective in photonic quantum information technology.

Introduction.—Quantum simulation of complex many-body problems, such as Bose-Einstein condensation and superfluid (SF) to Mott-insulator (MI) quantum phase transition (QPT), has been one of the central themes of atomic physics and condensed matter physics for the past few decades [1]. Recently, the possibility of implementing similar Hamiltonians based on cavity polaritons, a quasiparticle consisting of elementary excitation of light and matter, has been investigated theoretically. The QPT from a SF to MI state was predicted in a variety of systems such as a cavity array containing four-level

atomic ensembles in an EIT configuration [2], single-atom cavity QED array [3,4], and excitonic cavity QED array [5]. The existence of Bose-glass (BG) phase [5,6] and certain magnetic order [7,8] were also predicted. Most of these proposals rely on a cavity QED system in the strong coupling regime and require a large array of coupled ultrahigh- Q cavities. Unlike ultracold atoms in an optical lattice where an extremely clean experimental environment can be prepared, disorder due to the fabrication error of solid-state devices is unavoidable and therefore the study on the robustness against system imperfection is crucially important [5]. In this letter, we propose that a polaritonic QPT finds unique applications for massive parallel generation of indistinguishable single photons and polarization-entangled photon-pairs on demand. We will show that the proposed system does not require an ultrahigh- Q cavity and is robust against fabrication error. Such a nonclassical photon source could potentially open up a new perspective in quantum computation, communication, metrology, simulation and lithography.

Fig. 1 shows a basic device based on a periodically modulated semiconductor planar microcavity with a single quantum well (QW) inserted in the optical cavity layer that is in between the upper and lower distributed-bragg-reflectors (DBR). The cavity photons are laterally trapped by locally increasing the optical cavity layer thickness [9], and the QW excitons are laterally trapped by applying a vertical electric field [10]. The dynamics of such an array of exciton-polariton traps can be described by the Bose-Hubbard model with a system-reservoir coupling (see *Hamiltonian and Master Equation* below). By carefully designing a coherent optical pumping followed by a photon-exciton frequency detuning switching, indistinguishable single photons and polarization-entangled photon-pairs can be extracted on demand. More importantly, the system disorder is shown to

have a limited influence on the device performance. Our system exhibits a very large polariton-polariton on-site nonlinear interaction due to the exciton-exciton repulsive interaction through Coulomb exchange and the effective reduction of dipole moment through phase space filling [11,12]. The modulated planar microcavities inherit circular symmetry and are suitable for coupling to down-stream fiber-optics with high collection efficiency.

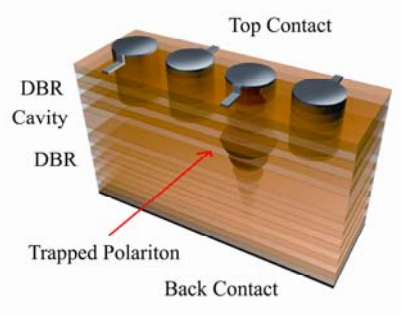


FIG. 1. The proposed device based on a periodically modulated planar microcavity (not to scale). A single GaAs QW (not shown) is embedded in a $\lambda/2$ $\text{Al}_x\text{Ga}_{1-x}\text{As}$ optical cavity layer, which is sandwiched between the upper and lower DBR. The DBR consists of alternating AlAs/GaAs $\lambda/4$ plates. The whole structure is grown on a GaAs substrate (not shown) where metal contacts are fabricated on the top and bottom surfaces. The lower DBR is made thicker than the upper DBR to enforce single-side cavity emission.

Hamiltonian and Master Equation.—The system Hamiltonian is described by

$$\begin{aligned}
H = & \int d\mathbf{r} \Psi_a^\dagger(\mathbf{r}) \left(\frac{-\nabla^2}{2m_a} + V_a(\mathbf{r}) \right) \Psi_a(\mathbf{r}) + \int d\mathbf{r} \Psi_b^\dagger(\mathbf{r}) \left(\frac{-\nabla^2}{2m_b} + V_b(\mathbf{r}) \right) \Psi_b(\mathbf{r}) \\
& + g' \int d\mathbf{r} \Psi_a^\dagger(\mathbf{r}) \Psi_b(\mathbf{r}) + H.c. \\
& + \frac{u'}{2} \int d\mathbf{r} \Psi_b^\dagger(\mathbf{r}) \Psi_b^\dagger(\mathbf{r}) \Psi_b(\mathbf{r}) \Psi_b(\mathbf{r}) \\
& - s' g' \int d\mathbf{r} \Psi_b^\dagger(\mathbf{r}) \Psi_a^\dagger(\mathbf{r}) \Psi_b(\mathbf{r}) \Psi_b(\mathbf{r}) + H.c. \\
& + \int d\mathbf{r} f'(\mathbf{r}, t) e^{-i\omega t} \Psi_a^\dagger(\mathbf{r}) + H.c.
\end{aligned} \tag{1}$$

where subscripts a and b refer to cavity photon and QW exciton, respectively. The first and second terms in (1) are the free Hamiltonians of trapped photons and excitons. The third through sixth terms correspond to photon-exciton coupling, exciton-exciton repulsive interaction, effective reduction of dipole moment, and the external laser drive, respectively. Here we assume the optical cavity layer thickness and vertical electric field are appropriately implemented so that both the cavity photon and QW exciton wavefunctions are localized within a length scale $\lambda = 800$ nm (emission wavelength of a 10 nm GaAs QW) / 3.6 (GaAs refractive index). The required trapping potentials should be much larger than 193.9 and 63.7 μeV , which are the photon and exciton kinetic energies respectively. The corresponding local increase of optical cavity layer thickness is about $\lambda/2$ [9], and the corresponding strength of vertical electrical field is around 30 kV/cm [10]. Next, we define the upper polariton (UP) and lower polariton (LP) operators as a linear superposition of the photon and exciton operators with appropriate Hopfield coefficients A and B , respectively. The system master equation for LPs in the rotating frame of external laser drive is derived as

$$\frac{d\rho}{dt} = \frac{1}{i}[\tilde{H}, \rho] - \frac{\Gamma}{2} \sum_i (\rho p_i^\dagger p_i + p_i^\dagger p_i \rho - 2p_i \rho p_i^\dagger) \quad (2)$$

where

$$\tilde{H} = -\Delta \sum_i p_i^\dagger p_i - J \sum_{\langle ij \rangle} p_i^\dagger p_j + \frac{U}{2} \sum_i p_i^\dagger p_i^\dagger p_i p_i + F(t) \sum_i (p_i^\dagger + p_i). \quad (3)$$

Δ is the energy difference between the external laser drive and a trapped LP. J is the LP tunneling energy and is equal to tA^2 , i.e., the photon tunneling energy t times the photon fraction of a LP A^2 . U is the LP-LP interaction energy and is equal to uB^4 (exciton-exciton repulsive interaction) plus $4sgB^3A$ (effective reduction of dipole moment). The

numerical values of u and sg are calculated to be 200 and 90 μeV [11,12]. $F(t)$ represents the external laser coupled to the cavity photon mode. Γ is the LP decay rate and is equal to $A^2\gamma_a$ (photon decay) plus $B^2\gamma_b$ (exciton decay). Realistic experimental parameters such as cavity Q factor equal to 10^6 and exciton lifetime equal to 0.5 ns are assumed. The system decoherence is limited by the radiative process because the acoustic phonon-polariton scattering is expected to exceed 1 ns for zero in-plane momentum regime at cryogenic temperature, and the polariton-polariton scattering is negligible for LP density smaller than 10^{10} cm^{-2} . UP dynamics are neglected because an external laser selectively pumps the LP. Notice that the photon-exciton coupling constant has to be the dominant energy scale for the above polaritonic picture works properly. This is justified because g is about 2.5 meV [13] and is at least an order of magnitude larger than the other relevant energy scales in the following simulations.

Generation of Indistinguishable Single Photons.—We perform a direct time-domain simulation based on the master equation (2) to study LP dynamics. Due to limited computational resource, we assume 4 one-dimensional coupled cavities with periodic boundary conditions. The number of basis that spans the Hilbert space is chosen in a way that at most 4 LPs can be excited. The finite size effect would influence the particle statistics and the QPT critical point, but the underlying physics remains unchanged. The basic device operation procedure is shown in fig. 2 (a) and (b) for the odd (1, 3) and even (2, 4) numbered cavities, respectively. The system is initially prepared in a deep SF state where $U/J \sim 0.13$, which is realized by a red photon-exciton frequency detuning $\delta = -3g$. t is set to be 20 GHz. An optical pump pulse is then resonantly injected so that the ground state LP population rises to 4 during the time window from 0 to 50 ps. Then, due to

quantum-confined Stark effect, the exciton energy is lowered by the applied vertical electric field so that δ is switched from $-3g$ to $4g$, i.e., into a deep MI state where $U/J \sim 35$. A single polariton is trapped per cavity now. The shape of an electrical switch pulse follows a hyperbolic tangential function with switching speed equal to 10 GHz, which is chosen to perform an adiabatic QPT during the time window from 50 to 250 ps. Finally, while δ of the even numbered cavities stay at $4g$, δ of the odd numbered cavities are rapidly switched at the speed of 1 THz back to $-4g$, i.e., $U/J \sim 0.20$ at 250 ps. Notice that γ_b and g are independent of δ because the lifetime and oscillator strength of an exciton change barely for the range of vertical electric field used in the above δ switching [10].

The dual electric field control triggers single photon emission under three considerations. First, the quantum efficiency of generating single photon [14,15,16]

$$\eta = \int \langle p_i^\dagger(t) p_i(t) \rangle A^2(t) \gamma_a dt \quad (4)$$

should be maximized so that a polariton decay is mostly channeled to the cavity photon mode. Switching the exciton-like LP back to photon-like LP achieves this goal. Second, if all of the cavities are switched back to a large red detuning regime, rapid tunneling process with $J/\Gamma \sim 194$ readily destroys the deterministic single polariton decay from individual site. Instead, in the present selective switching scheme, only the LPs in the odd numbered cavities are switched back to a large red detuning regime so that the neighboring site energy mismatch effectively cuts off the tunneling events. Finally, the frequency of the emitted single photons from the odd numbered cavities is tuned away from that of the external laser drive. Using a narrow band-pass frequency filter, clean output signal can be selected out.

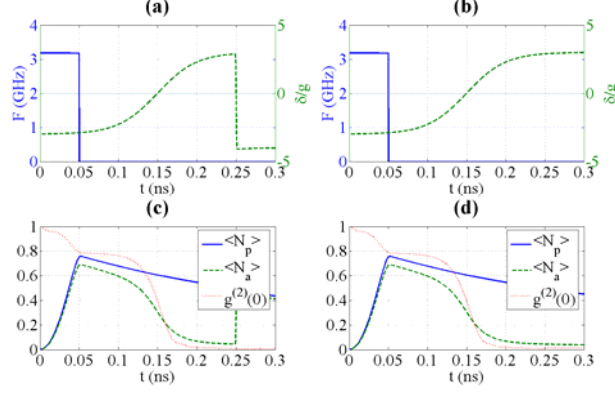


FIG. 2. The basic device operation procedure and LP dynamics in the odd (a) (c) and even (b) (d) numbered cavities plotted as a function of time. The solid-blue and dashed-green lines in (a) (b) are the optical pump pulse and electrical switch pulse, respectively. In (c) (d), the solid-blue, dashed-green, and dotted-red lines corresponds to the average LP number, average photon number, and LP second-order coherence.

The dynamics of the odd and even numbered cavities are plotted in fig. 2 (c) and (d), where the average number of polaritons $\langle N_p \rangle$ and photons $\langle N_a \rangle$ are plotted. During QPT, the normalized zero-delay second-order coherence function $g^{(2)}(0)$ starts with about 0.8 rather than 1 at 50 ps due to the finite size effect, and subsequently drops to about 0.007 at 250 ps. This strongly antibunching behavior indicates the QPT from a SF to MI state. The effect of dual electric field control can be seen from the sharp increase of $\langle N_a \rangle$ in the odd numbered cavities. η of the single photon emission is about 61% in fig. 2, and can be enhanced to 85% using a shorter pump pulse accompanied with a faster adiabatic δ switching rate and a smaller cavity Q factor. Further maximization is possible by carefully designing the pump and switch pulse shapes. The ultimate limit of η comes from how large U can be and therefore how fast an adiabatic δ switching may use.

To further understand the system dynamics, we define two parameters: the far-field optical interference visibility [17]

$$V(t) \equiv \frac{\langle n_a(t) \rangle_{\max} - \langle n_a(t) \rangle_{\min}}{\langle n_a(t) \rangle_{\max} + \langle n_a(t) \rangle_{\min}} \quad (5)$$

where

$$n_a(t) = \frac{1}{N} \sum_{m,n} a_m^\dagger(t) a_n(t) e^{i(m-n)\phi} \quad (6)$$

and the single photon indistinguishability [18]

$$I(t) \equiv 1 - \frac{\langle c_1^\dagger(t) c_3^\dagger(t) c_3(t) c_1(t) \rangle}{\langle c_1^\dagger(t) c_1(t) \rangle \langle c_3^\dagger(t) c_3(t) \rangle} \quad (7)$$

where

$$\begin{pmatrix} c_1 \\ c_3 \end{pmatrix} = \frac{1}{\sqrt{2}} \begin{pmatrix} 1 & 1 \\ -1 & 1 \end{pmatrix} \begin{pmatrix} a_1 \\ a_3 \end{pmatrix}. \quad (8)$$

The visibility $V(t)$ measures the first-order phase coherence through the far-field optical interference contrast. The indistinguishability $I(t)$ measures the identity of the two photons emitted simultaneously from the two cavities through the Hong-Ou-Mandel interferometer. These quantities are plotted as a function of time in fig. 3. As expected, I rises to nearly 1 after entering into a MI state, suggesting the generation of indistinguishable single photons. On the other hand, V drops from 1 to only 0.36 rather than 0 at the end. Such a non-vanishing visibility originates from the following scenario: to achieve an adiabatic QPT from a SF to MI state, the LP tunneling rate has to be larger than its decay rate for the system to reach equilibrium [5]. As a result, in the MI phase where $J/\Gamma \sim 5.6$, after a single photon is emitted from a particular site the LPs in the nearby cavities have small but finite chance to hop into the empty cavity and consequently create extra phase coherence. Such an example shows the system-reservoir

coupling has non-negligible effect and a thermal equilibrium picture doesn't fully apply. Notice that by using a smaller t or Q , the final visibility can be further decreased.

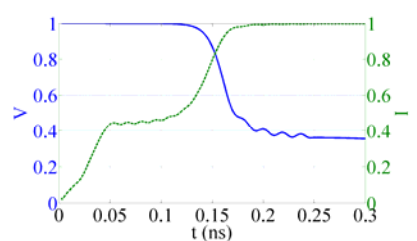


FIG. 3. The far-field optical interference visibility (solid-blue line) and the single photon indistinguishability (dashed-green line) plotted as a function of time. Only odd numbered cavities (1, 3) are taken into calculations. The slight oscillations in both parameters are caused by a moderate δ switching speed.

System Disorder.—To study the impact of unavoidable system imperfection, we introduce small deviations in exciton site energies as $+d, 0, -d, 0$ for cavity number 1 to 4. One important benefit of our proposal is its robustness against such a system disorder. First, a vertical electric field control can be used to correct the inhomogeneous site energies by applying appropriate voltages. Second, because we inject the LPs into the system prepared in a SF state, the site energy disorder is effectively reduced by roughly a factor of d/J . Such an effect is shown by plotting the single photon indistinguishability as a function of exciton site energy disorder in fig. 4. $I \sim 1$ maintained up to $d \sim 100 \mu\text{eV}$ and drops rapidly hereafter, which corresponds to the corruption of MI plateau completely by the appearance of BG states [5]. To compare the robustness of our system, we perform intensive numerical simulations on an array of photon blockade devices [19]. We find that for even $20 \mu\text{eV}$ of disorder, the indistinguishability drops swiftly in the photon blockade device array because the bandwidth of a pumped π pulse cannot well overlap the inhomogeneous LP site energies spectrally. The increase of a pumped π pulse

bandwidth to improve the spectral coupling is not allowed because a second LP is then excited and the photon blockade principle breaks down. Such a preliminary study shows that our scheme can largely overcome the residual site energy disorder such as inhomogeneous broadening of QW exciton and cavity photon, and therefore promises a practical path toward massive parallel generation of indistinguishable single photons.

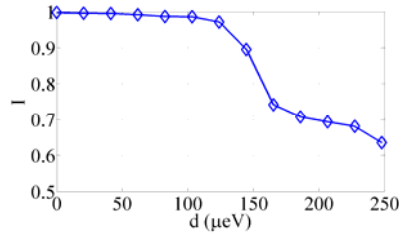


FIG. 4. The single photon indistinguishability plotted as a function of exciton site energy disorder.

Generation of Polarization-Entangled Photon-Pairs.— So far we have neglect the spin of a LP by assuming a circularly-polarized coherent optical pump is used. It is possible to generate polarization-entangled photon-pairs via the QPT from a SF to MI state if the two spin species are simultaneously injected. Our scheme is illustrated in fig. 5, where initially a linearly-polarized external laser injects in average two LPs per site in a photon-like SF state. Subsequent adiabatic δ switching sweeps the system into an exciton-like MI, where the ground state is two LPs with opposite spins occupying the same site. This is because of the weak attractive interaction between two polaritons with opposite spins. Using a dual electric field control as described above, two-photon cascaded emission is triggered where the anticorrelation of the LP spins is translated to the circularly-polarized state of the photons. A maximally polarization-entangled photon-pair $(|\sigma^+>_1|\sigma^->_2+|\sigma^->_1|\sigma^+>_2)/\sqrt{2}$ can be obtained, where subscripts 1 and 2 refer to the first and second photon emitted, which have an energy difference roughly equal to U . Such a

process is similar to the biexciton emission in a semiconductor quantum dot [20,21] where we take advantage of the QPT to simultaneously initialize the system. Notice that the QPT of filling factor equal to two occurs at $U/J \sim 7.69$ [22], which is within the reach of the proposed device operation as previously discussed.

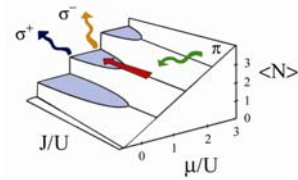


FIG. 5. Phase diagram of the Bose-Hubbard model (not to scale). The system is first pumped by a linearly-polarized (π) external laser, and then followed by a δ switching indicated by the red arrow. Subsequent dual electric field control triggers polarization-entangled photon-pairs that are circularly-polarized (σ).

Conclusion.—We have shown how to harness the polaritonic QPT from a SF to MI state to generate indistinguishable single photons and polarization-entangled photon-pairs. The system robustness against site energy disorder by means of pumping a SF state serves a practical application to various photonic quantum information processing. A variety of optical precision measurements such as photon number eigenstate interferometer [23] and subwavelength quantum lithography [24], are the other application area for the proposed scheme.

One of the authors (N. N.) was partially supported by Mediatek Fellowship. We would like to thank Q. Zhang for useful discussion. This work was supported by SORST program of Japan Science of Technology Corporation (JST), the University of Tokyo (CINQIE), and NTT Basic Research Laboratories.

- [1] I. Bloch, *Nature Phys.* **1**, 23 (2005).
- [2] M. J. Hartmann, F. G. S. L. Brandão, and M. B. Plenio, *Nature Physics* **2**, 849 (2006).
- [3] A. D. Greentree, C. Tahan, J. H. Cole, and L. C. L. Hollenberg, *Nature Physics* **2**, 856 (2006).
- [4] D. G. Angelakis, M. F. Santos, and S. Bose, *Phys. Rev. A* **76**, 031805(R) (2007).
- [5] N. Na, S. Utsunomiya, L. Tian, and Y. Yamamoto, *Phys. Rev. A* **77**, 031803(R) (2008).
- [6] D. Rossini and R. Fazio, *Phys. Rev. Lett.* **99**, 186401 (2007).
- [7] M. J. Hartmann, F. G. S. L. Brandão, and M. B. Plenio, *Phys. Rev. Lett.* **99**, 160501 (2007).
- [8] A. Ji, X. C. Xie, and W. M. Liu, *Phys. Rev. Lett.* **99**, 183602 (2007).
- [9] R. Idrissi Kaitouni, O. El Daïf, A. Baas, M. Richard, T. Paraiso, P. Lugan, T. Guillet, F. Morier-Genoud, J. D. Ganière, J. L. Staehli, V. Savona, and B. Deveaud, *Phys. Rev. B* **74**, 155311 (2006).
- [10] H.-J. Polland, L. Schultheis, J. Kull, E. O. Göbel, and C. W. Wu, *Phys. Rev. Lett.* **55**, 2610 (1985).
- [11] C. Ciuti, V. Savona, C. Piermarocchi, A. Quattropani, and P. Schwendimann, *Phys. Rev. B* **58**, 7926 (1998).
- [12] S. Schmitt-Rink, D. S. Chemla, and D. A. B. Miller, *Phys. Rev. B* **32**, 6601 (1985).
- [13] H. Deng, G. Weihs, C. Santori, J. Bloch, and Y. Yamamoto, *Science* **298**, 199 (2002).
- [14] C. K. Law and H. J. Kimble, *J. Mod. Opt.* **44**, 2067 (1997).
- [15] A. Kuhn, M. Hennrich, T. Bondo, and G. Rempe, *Appl. Phys. B* **69**, 373 (1999).

- [16] G. Cui and M. G. Raymer, *Opt. Express* **13**, 9660 (2005).
- [17] M. X. Huo, Y. Li, Z. Song, and C. P. Sun, *Phys. Rev. A* **77**, 022103 (2008).
- [18] A. Kiraz, M. Atatüre, and A. Imamoglu, *Phys. Rev. A* **69**, 032305 (2004).
- [19] A. Imamoglu, H. Schmidt, G. Woods, and M. Deutsch, *Phys. Rev. Lett.* **79**, 1467 (1997).
- [20] O. Benson, C. Santori, M. Pelton, and Y. Yamamoto, *Phys. Rev. Lett.* **84**, 2513 (2000).
- [21] R. M. Stevenson, R. J. Young, P. Atkinson, K. Cooper, D. A. Ritchie, and A. J. Shields, *Nature* **439**, 179 (2002).
- [22] G. G. Batrouni and R. T. Scalettar, *Phys. Rev. B* **46**, 9051 (1992).
- [23] M. J. Holland and K. Burnett, *Phys. Rev. Lett.* **71**, 1355 (1993).
- [24] A. N. Boto, P. Kok, D. S. Abrams, S. L. Braunstein, C. P. Williams, and J. P. Dowling, *Phys. Rev. Lett.* **85**, 2733 (2000).